

OPTIMAL IMPROVED PID CONTROLLER WITH GOA ALGORITHM FOR SINGLE LINK HUMAN LEG ROBOT

*Aliaa Adnan¹

Ekhlas H. Karam¹

1) Computer Engineering Department, College of Engineering, Mustansiriyah University, Baghdad, Iraq

Received 24/9/2021

Accepted in revised form 19/11/2021

Published 1/3/2022

Abstract: A Human Leg Robot (HLR) is a type of manipulator robot that has non-linear, quality, time-varying behaviors and uncertainty in parameters. Therefore, it must be controlled. The purpose of this work is to design an optimal Improved Proportional-Integral-Derivative (IPID) controller for this robot to improve its performance in tracking the desired path. Two schemes of IPID controllers are suggested to enhance the performance of the traditional PID in controlling the human leg robot and following the desired path. The Grasshopper Optimization Algorithm (GOA) is considered to optimize the IPID parameters. The performance of the suggested IPID structures has been compared to traditional PID methods. The simulation results show that the efficiency of these schemes was enough to handle the tracking problems of the HLR.

Keywords: *human leg robot, optimal Proportional-Integral-Derivative, grasshopper optimization algorithm*

1. Introduction

Robot manipulators are crucial in modern industry because they reduce manufacturing costs and improve precision, quality, productivity, and efficiency. Controlling robot manipulators is difficult due to their nonlinear, linked, and time-varying characteristics. Furthermore, there are always uncertainties in the dynamic model of the system, such as external disturbances and parameter uncertainty, which

cause the robot manipulator systems to operate in an unstable manner.

In spite of several control algorithms for robot manipulators, PID control remains one of the preferred methods in many actual robot systems [1]. The key reason is that the notion is intuitive, and the PID design is simple. In this way, PID controls are the simplest and most efficient solution to a wide range of real-world automated control challenges. Furthermore, PID regulators are the foundation of most industrial control systems. The main reason for using a PID controller is that it is based on a strong educational foundation in control theory.

In summary, the derived procedure is known as improving the closed-loop system's dynamics, whereas the integrated procedure is known as removing the steady-state error and improving low-frequency reference tracking [2]. As a result, a number of papers have addressed the PID control of robotic manipulators [3, 4]. By using a typical PID control strategy for robotic systems, they will encounter at least two major drawbacks. First, since the feedback gains of a conventional PID controller are usually constant, the overall

*Corresponding Author: aliaaadnan96@gmail.com

performance of a closed-loop system may be poor in the presence of dynamic uncertainty or external disturbances. Many technologies have been developed to address this issue, such as genetic algorithms, fuzzy logic, neural networks, and particle swarm optimization, to enable autonomous PID gain adjustment [5-7].

Integrating such methods, on the other hand, can add to the overall controller's complexity. Second, stability has always been a big worry with PID control in robotic systems, because unmolded dynamics or disturbances are prone to driving the system out of its stated stability regime.

The literature shows that PID controllers have been improved using several methods. In [8], a hybrid PD-PID controller has been developed for two-link flexible manipulator systems. The authors [9] have presented a new modified PID hybrid fuzzy controller for robot manipulators that provides high performance nonlinear methodology.

An optimal improved PID controller is suggested in this paper for a single-link Human Leg Robot (HLR). This controller consists of an optimal PID controller and a feed-forward controller. The details of this controller will be explained in the sections of this paper.

The rest of the paper is organized as follows: The dynamics of HRL are presented in Section 2. The proposed control scheme is described in Section 3. GOA is described in Section 4. Simulation results and discussion are presented in Section 5. Concluding remarks are given in Section 6.

2. Dynamic Model of the Single Link HLR

The human leg robot (HLR) can be modeled depending on the relationship between the output of the angular rotation around the hip joint and the input torque that is generated by the muscles of the leg [10]. Figure (1) shows a cylindrical

model of a simplified human leg robot. The parameters of this model are defined by Table (1).

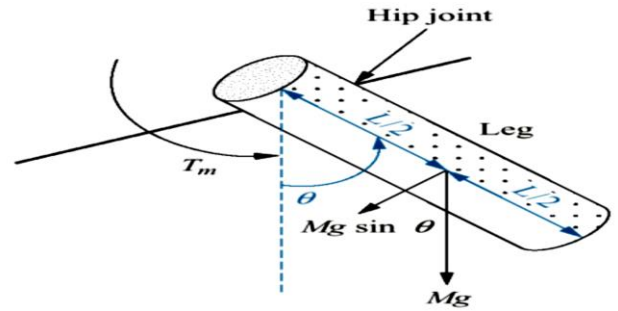


Figure 1. Cylindrical model of a simplified human leg robot [11].

Table 1. The description of HLR model parameters.

Symbol	Description	Value
L :	the length of the leg and the weight can be determine as $L/2$.	0.5 m
D :	viscous damping.	0.1 Nms/rad
M :	mass of the leg.	1 kg
J :	inertia around the hip joint.	0.4 kgm ² /s ²
g :	acceleration due to gravity creates a nonlinear torque.	9.81
T_m :	torque supplied by DC motor	---
L :	the length of the leg and the weight can be determine as $L/2$.	---

The nonlinear dynamic model equation of this robot can be written as follows [11, 12, and 13]:

$$J \frac{d^2\theta}{dt^2} + D \frac{d\theta}{dt} + Mg \frac{L}{2} \sin \theta = T_m(t) \quad (1)$$

Where $(\frac{d^2\theta}{dt^2})$ term is the inertia torque, $D \frac{d\theta}{dt}$ term is the damping torque, and $Mg \frac{L}{2} \sin \theta$ term is the component of weight.

With small angle approximation, Eq. (1) can be linearized, where the θ variation is small, therefore the $\sin \theta$ term can be approximated to θ , and hence Eq. (1) becomes:

$$J \frac{d^2\theta}{dt^2} + D \frac{d\theta}{dt} + Mg \frac{L\theta}{2} = T_m(t) \quad (2)$$

$$\frac{\theta(s)}{T_m(s)} = \frac{1/J}{s^2 + \frac{D}{J}s + \frac{MgL}{2J}} \quad (3)$$

By substituting, the parameters of Table (1), the Eq. (3) becomes:

$$G_r(s) = \frac{\theta(s)}{T_m(s)} = \frac{2.5}{s^2 + 0.025s + 6.131} \quad (4)$$

This transfer function has two complex poles: $-0.0125 + 2.4761j$, $-0.0125 - 2.4761j$.

3. The Suggested Improved PID Controller

Two schemes of an improved PID (IPID) controller are suggested in this paper to make the HLR follow the desired position accurately. These schemes consist of two parts. The first part is an optimal PID controller, while the second part is a forward controller. The term "feed-forward" was coined in the early years of the development of the control systems field as an intuitive name to refer to the counterpart of the feedback used in closed-loop systems. Additionally, it is a block that connects the input of the control system to the input of the controlled plant, as depicted in Figures (2) and (3). The feed-forward block is used as a tool to eliminate disturbances to the plant coupled with feedback control [14]. The forward controller is added to enhance the performance of the optimal PID in controlling the HLR to follow the desired trajectory. The GOA tunes the parameters of the optimal PID part of these schemes and the parameters of the desired model. The following subsections explain these two schemes in more detail.

3.1. Improve PID Scheme I (IPID-SI)

The block diagram of this scheme is shown in Figure (2).

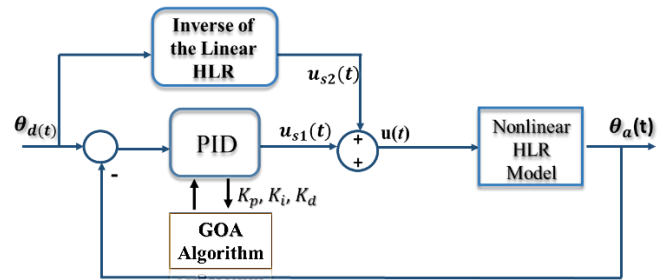


Figure 2. The block diagram of the IPID-S1.

This controller consists of the optimal PID and a feed-forward controller, so the overall controller becomes:

$$u(t) = u_{s1}(t) + u_{s2}(t) \quad (5)$$

The equation of $u_{s1}(t)$ is:

$$u_{s1}(t) = K_p e(t) + K_i \int_0^t e(t) dt + K_d \frac{de(t)}{dt} \quad (6)$$

Where K_p is a proportional gain, K_i is an integral gain, and K_d is a derivative gain. The $e(t)$ is the error signal, which is the difference between the desired angle and the actual leg output angle. GOA determines the parameters of K_p , K_i , and K_d . The feed-forward controller represents the improvement part of the optimal PID. This controller is chosen to be equal to the inverse of the equation of the linear robot model. Therefore, the equation is:

$$u_{s1}(t) = g_r(t)^{-1} \quad (7)$$

3.2. Improve PID Scheme II (IPID-SII)

The block diagram of this scheme is shown in Figure (3), where the optimal PID is sum with the feed-forward controller, the control law of this scheme is:

$$u_c(t) = u_{x1}(t) + u_{x2}(t) \quad (8)$$

Where $u_{x1}(t)$ is an optimal PID (Eq.(6)), while a feed-forward part is chosen equal to the inverse of a desired second order linear equation, the desired equation is:

$$D(s) = \frac{\omega_n^2}{s^2 + 2\xi\omega_n s + \omega_n^2} \quad (9)$$

Where ω_n is natural frequency, ξ is damping ratio. The parameters of (ω, ξ) and the optimal PID controller are tuned by the GO algorithm.

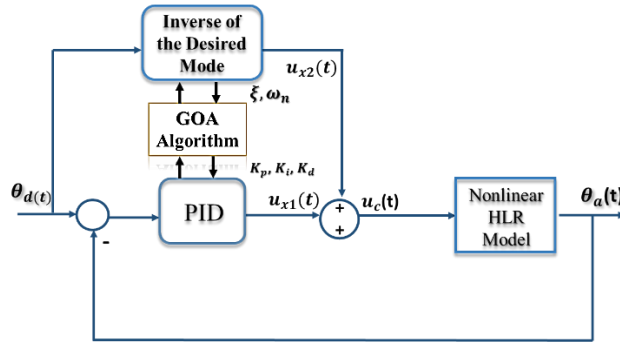


Figure 3. The block diagram of the IPID-SII1.

4. Grasshopper Optimization Algorithm

Saremi et al. introduced the GOA algorithm in [14], which is a new and fascinating swarm intelligence algorithm that simulates grasshopper foraging and swarming behavior. Grasshoppers are insects that cause havoc on crop production and agriculture [15, 16]. Their life cycle is divided into two stages: nymph and adulthood. Small steps and moderate movements describe the nymph phase, whereas long-range and rapid movements represent the maturity phase [15].

Nymph and adult motions define the intensification and divarication phases of GOA. The mathematical model for grasshopper swarming behavior is as follows [15, 16]:

$$X_i = S_i + W_i + Z_i \quad (10)$$

In the above equation, X_i represents the grasshopper's i^{th} position, S_i represents social participation, W_i represents gravitational force over a grasshopper, and Z_i represents air-advection. In the preceding equation, randomness is produced by:

$$X_i = h_1 S_i + h_2 W_i + h_3 Z_i \quad (11)$$

Where h_1, h_2 and h_3 are random numbers between zero and one. S_i is designed as follows:

$$S_i = \sum_{\substack{j=1 \\ j \neq i}}^N s(d_{ji}) \widehat{d}_{ji} \quad (12)$$

The distance between i^{th} and j^{th} grasshopper is computed using Eq. (13).

$$d_{ji} = |x_j - x_i| \quad (13)$$

In addition:

$$\widehat{d}_{ji} = \frac{x_j - x_i}{d_{ji}} \quad (14)$$

Moreover, the strength of the social forces is described in Eq. (15).

$$s(r) = F y^{\frac{-d}{l}} - y^{-d} \quad (15)$$

Where F denotes the attractive force, d denotes the distance, and l denotes the attraction measure. Eq. (10) represents the W component and can be written as:

$$W_i = -b \hat{y}_b \quad (16)$$

Where b is the gravitational force, the negative sign shows its orientation toward the center of the earth, while \hat{y}_b is the unit vector toward the earth.

Now, the Z component in Eq. (10) is given as:

$$Z_i = c \hat{y}_w \quad (17)$$

Where c is the continuous wind drift and \hat{y}_w shows the wind direction unit vector. By putting the values of $S, W,$ and Z into Eq. (10), we get:

$$X_i = \sum_{\substack{j=1 \\ j \neq i}}^N s(|x_j - x_i|) \frac{x_j - x_i}{d_{ji}} - b \hat{y}_b + c \hat{y}_w \quad (18)$$

The swarm in the free space equation above is used in simulation to describe the interaction of grasshoppers in a swarm. The flowchart for the GOA is given in Figure (4). The cost function used in this research is ITSE (Integral Time-

weighted Squared Error), which is described by the following equation:

$$\text{Fitness} = \text{ITSE} = \int_0^t t * \text{Error}(t)^2 \tag{19}$$

Where *Error* is the error between the desired input and the response in each link.

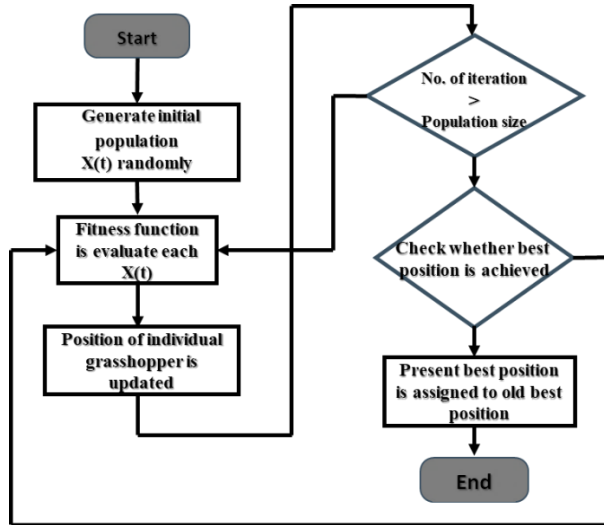


Figure 4. Flowchart the GOA algorithm.

5. Simulation Results

The simulation results of the traditional optimal PID and the suggested IPID schemes based on the GO algorithm have been presented for controlling the position of the single link HLR nonlinear model using the MATLAB program. In this section, the results of two paths for the position of the robot are tested: the linear and the non-linear path. In order to investigate the robustness of control, a nonlinear sinusoidal (0.01sin (5t)) disturbance is included with the HLR model.

The parameters of the GOA that are considered are given in Table (2), and hence the optimal parameters that are obtained by GOA for the traditional PID, IPID-S1, and IPID-SII schemes are listed in Table (3).

Table 2. The parameters of the GOA.

GOA parameters	Value
Number of search agents	25
Max iteration	5
intensity of attraction (f)	0.5
attractive length scale (l)	1.5

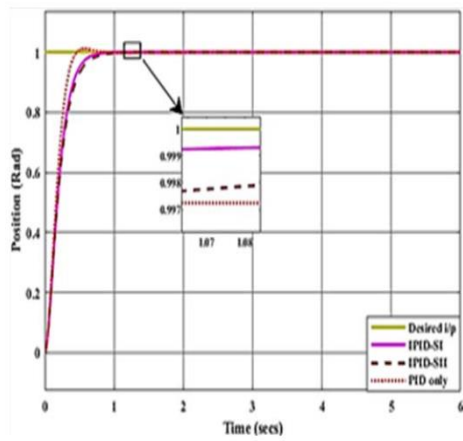
Table 3. Optimal parameters of the PID, IPID-SI, and IPID-SII.

Controller	PID	IPID-SI	IPID-SII
K_p	34.3695	49.6709	4.6673
K_i	11.2689	3.7446	7.8907
K_d	5.9994	11.0822	1.5506
ξ	---	---	8.5749
ω_n	---	---	8.5749

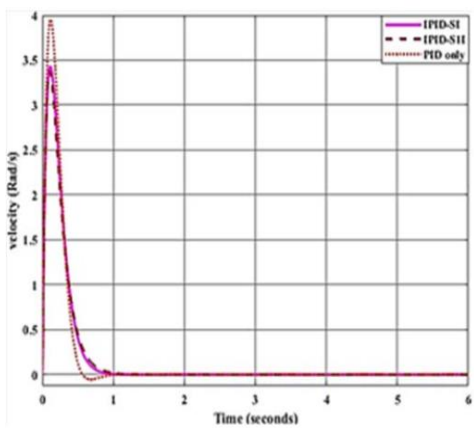
The simulation results of HLR for the linear unit step desired angle (position, velocity, and control signal) are shown in Figure (5), and the comparing evaluation of PID, IPID-SI, and IPID-SII results are shown in Table (4). These results show that all the controllers (PID, IPID-SI, IPID-SII) improved the performance of the HLR with fast response (small settling time t_s), nearly zero error steady state $e_{s,s}$, minimum or no oscillation (maximum peak $M_p\% < 1.1$), maximum torque ($M_T < 35 \text{ N/m}$) spatially with the suggested IPID-SI, IPID-SII which gives more improvement than the PID controller as illustrated in Figure (6) and Table 4.

Table 4. The evaluation parameters of the traditional PID and the suggested controller.

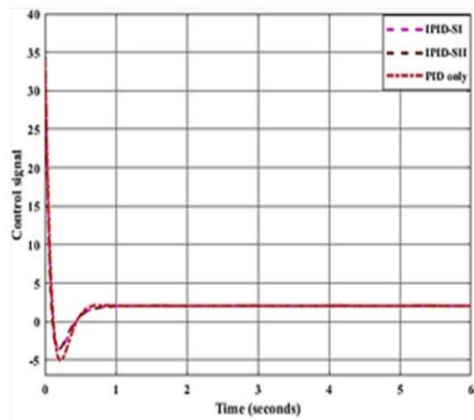
Parameters	IPID-SI	IPID-SII	PID
M_p (%)	0	0	1.0870
t_s	0.6153	0.695	0.4103
$e_{s,s}$	0.0004	0.0003	-0.0001
$t_r(sec.)$	0.3553	0.3871	0.2668



(a)



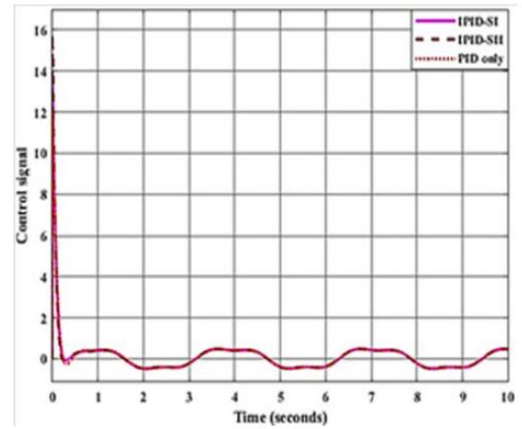
(b)



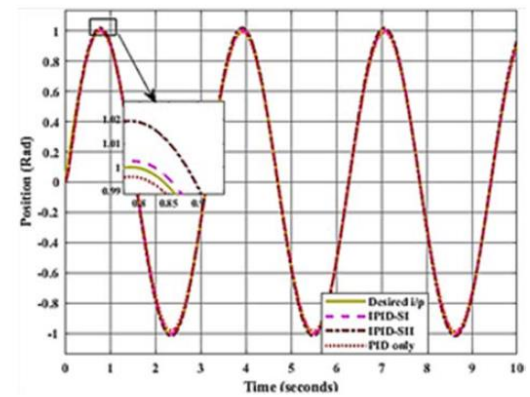
(c)

Figure 5. Simulation results of the HLR model with the suggested controllers (a) output position, (b) output velocity and (c) the control signal.

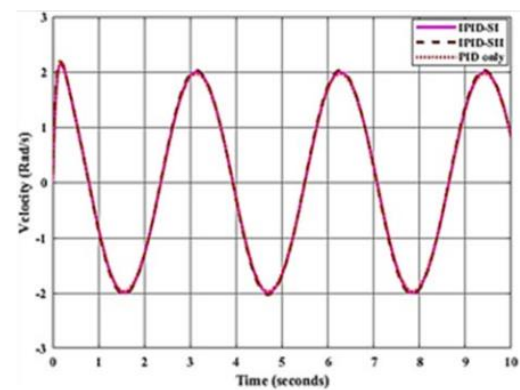
The simulation results of HLR for the nonlinear sinusoidal desired angle (position, velocity, and control signal) are shown and compared with PID, IPID-SI, and IPID-SII in Figure (6).



(a)



(b)



(c)

Figure 6. Simulation results of the HLR model with the suggested controllers (a) output position, (b) output velocity and (c) the control signal.

It can be noticed from Figure (6) that all the controllers satisfy the design requirement by making the robot system follow the nonlinear path (desired position and velocity) with fast response, very small or zero error, no overshoot, and maximum torque ($M_T < 16$ N/m) spatially with the suggested IPID-SI and IPID-SII.

The simulation results of both linear and nonlinear paths illustrate the efficiency of the suggested IPID-SI and IPID-SII models. In particular, the IPID-SI spatially feed-forward controller depends on the linear HLR model.

6. Conclusion

This paper focuses on suggesting two different optimal improved PID control schemes (IPID-SI and IPID-SII) to improve the performance of the HLR robot in tracking the required paths. The GO algorithm was used to improve the properties of the suggested control schemes. Through the simulation results of the controlled HLR, the IPID schemes showed better performance with fast response and efficiency in addressing the tracking problems under disturbance compared to the traditional optimal PID controller, spatially IPID-SI.

Acknowledgements

All thanks and appreciation to my supervisor, Ekhlash H. Karam, and those who helped me in providing advice to me to submit this research.

Conflict of interest

The authors confirm that the publication of this article does not cause any conflict of interest.

7. References

1. C. H. Aung, K. T. Lwin, and Y. M. Myint. (2008), “*Modeling Motion Control System for Motorized Robot Arm using MATLAB*”, World Academy of Science,

- Engineering and Technology, no. 3, pp. 372–375.
2. A. R. Ridwan, M. I. S. Bony, and I. I. Azad. (2012), “*Performance Analysis of MPC in the Control of a Simple Motorized Nonlinear Model of a Robotic Leg*”, International Journal of Computer Applications, vol. 54, no. 11, pp. 19–23.
3. C. Lauretti et al. (2018), “*Learning by demonstration for motion planning of upper-limb exoskeletons*”, Front in Neurobot, vol. 12, pp. 1–14.
4. K. J. Astrom and R. M. Murray. (2007), “*Feedback Systems*”, an Introduction for Scientists and Engineers, pp. 1-408.
5. S. A. Ajwad, J. Iqbal, M. I. Ullah, and A. Mehmood. (2015), “*A systematic review of current and emergent manipulator control approaches*”, Frontiers of Mechanical Engineering, vol. 10, no. 2, pp. 198–210.
6. D. Zhang and B. Wei. (2017), “*A review on model reference adaptive control of robotic manipulators*”, Annual Reviews in Control, pp. 1–11.
7. B. Nagaraj and N. Muruganath. (2010), “*A comparative study of PID controller thning using GA, EP, PSO and ACO*”, In 2010 International Conference on Communication Control and Computing Technologies, pp. 305–313.
8. J. Armendariz, V. Parra-Vega, R. García-Rodríguez, and S. Rosales. (2014), “*Neuro-fuzzy self-tuning of PID control for semiglobal exponential tracking of robot arms*”, Applied Soft Computing, vol. 25, pp. 139–148.
9. A. Belkadi, H. Oulhadj, Y. Touati, S. A. Khan, and B. Daachi. (2017), “*On the robust PID adaptive controller for exoskeletons: A particle swarm optimization based approach*”, Applied Soft Computing, pp. 1–28.

10. B. Wei. (2018), “*Adaptive control design and stability analysis of robotic manipulators*”, *actuators*, vol. 7, no. 4, pp. 1-17.
11. A. R. Ridwan, M. I. S. Bony, and I. I. Azad. (2012), “*Performance Analysis of MPC in the Control of a Simple Motorized Nonlinear Model of a Robotic Leg*”, *International Journal of Computer Applications*, vol. 54, no. 11, pp. 19–23.
12. R. L. Shell and E. L. Hall. (2000), *Handbook of Industrial Automation*, CRC press.
13. Karam, Ekhlas H., Ayam M. Abbass, and Noor S. Abdul-Jaleel. (2018), “*Design of Hybrid Neural Fuzzy Controller for Human Robotic Leg System*”, *Al-Khwarizmi Engineering Journal*, vol. 14, no. 1, pp. 145-155.
14. Thomas E. Marlin. (2015), *Process Control: Designing Processes and Control Systems for Dynamic Performance Modelling*, *Chemical Engineering Series, McGraw-Hill, New York*, pp. 78-79.
15. S. Saremi, S. Mirjalili, and A. Lewis. (2017), “*Grasshopper Optimisation Algorithm: Theory and application*”, *Advances in Engineering Software*, vol. 105, pp. 30–47.
16. A. A. Ewees, M. A. Elaziz, Z. Alameer, H. Ye, and Z. Jianhua. (2020), “*Improving multilayer perceptron neural network using chaotic grasshopper optimization algorithm to forecast iron ore price volatility*”, *Resources Policy*, vol. 65, pp. 1-12.